

measured rapid exchange rates for a transcription factor on a specific regulatory element in living cells. It is unclear whether any of the various factors recruited to a regulatory site remain statically bound.

The continuous exchange of liganded receptor with genomic targets is likely to have important consequences for physiologic responses of the cell. Many receptor responses are modulated by multiple cellular signaling pathways. For example, phosphorylation events mediated through independent protein kinase cascades can quickly alter the receptor-mediated expression level at a variety of promoters. Rapid exchange of a nuclear receptor with regulatory sites may facilitate the action of these secondary pathways because the receptor would be continuously available for modification, even in the presence of ligand.

The success of these experiments now opens the possibility of studying the direct interaction of many receptor coactivators and other receptor interaction activities with a natural gene target in real time in living cells. Further enhancements of this approach will likely lead to the ability to directly study molecular interactions at target regulatory regions through the application of fluorescent energy transfer (18) and proximity imaging of GFP-labeled factors (18).

References and Notes

1. H. Gronemeyer, in *Steroid Hormone Action*, M. G. Parker, Ed. (Oxford Univ. Press, New York, 1993), p. 94; M. G. Parker, *Curr. Opin. Cell Biol.* **5**, 499 (1993); N. J. McKenna, R. B. Lanz, B. W. O'Malley, *Endocr. Rev.* **20**, 321 (1999); L. Xu, C. K. Glass, M. G. Rosenfeld, *Curr. Opin. Genet. Dev.* **9**, 140 (1999).
2. T. E. Spencer et al., *Nature* **389**, 194 (1997); C. A. Hassig, T. C. Fleischer, A. N. Billin, S. L. Schreiber, D. E. Ayer, *Cell* **89**, 341 (1997); D. Chen et al., *Science* **284**, 2174 (1999).
3. C. Muchardt and M. Yaniv, *EMBO J.* **12**, 4279 (1993); S. K. Yoshinaga, C. L. Peterson, I. Herskowitz, K. R. Yamamoto, *Science* **258**, 1598 (1992); H. Chiba, M. Muramatsu, A. Nomoto, H. Kato, *Nucleic Acids Res.* **22**, 1815 (1994); C. J. Fryer and T. K. Archer, *Nature* **393**, 88 (1998).
4. P. Becker, R. Renkawitz, G. Schutz, *EMBO J.* **3**, 2015 (1984).
5. G. Rigaud, J. Roux, R. Pictet, T. Grange, *Cell* **67**, 977 (1991).
6. M. Truss, G. Chalepakis, M. Beato, *J. Steroid Biochem. Mol. Biol.* **43**, 365 (1992).
7. C. S. Suen et al., *J. Biol. Chem.* **273**, 27645 (1998).
8. D. Walker, H. Htun, G. L. Hager, *Methods* **19**, 386 (1999); P. Kramer et al., *J. Biol. Chem.* **274**, 28590 (1999).
9. G. L. Hager, in *Green Fluorescent Protein*, vol. 302 of *Methods in Enzymology*, M. P. Conn, Ed. (Academic Press, San Diego, CA, 1999), p. 73; H. Htun, J. Barsony, I. Rensyi, D. J. Gould, G. L. Hager, *Proc. Natl. Acad. Sci. U.S.A.* **93**, 4845 (1996).
10. The 3617 cell line is aneuploid and chromosome 4 varies in copy number, even in the haploid state. Thus, some of the cells in the population may not score for the LTR array because they are missing that copy of chromosome 4.
11. A. Belmont and colleagues [C. C. Robinett et al., *J. Cell Biol.* **135**, 1685 (1996)] developed a system in which a GFP-tagged lac repressor was shown to bind highly amplified copies of the lac operator element that was integrated in the chromosomes of CHO cells. They have used that system to study chromosome dynamics during the cell cycle. Others [I. Carmi, J. B. Kopynski, B. J.

Meyer, *Nature* **396**, 168 (1998)] have detected the interaction of transcription factors with amplified binding sites through immunofluorescence. A strength of the approach described here is that it uses an intact mammalian promoter with no alteration of the promoter and its associated regulatory elements. A somewhat surprising finding is that the density of GR-binding sites in the 3617 array is sufficiently high to permit easy detection of GFP-GR binding to the response elements. The arrays described by Belmont and colleagues contain a simple, highly reiterated lac operator sequence with a density of binding sites about two orders of magnitude higher than used here.

12. FRAP experiments (Fig. 5, A to F) were carried out as follows. A beam of light using the 488- and 514-nm laser lines was focused on the tandem array structure (Fig. 5A) in live cells after hormone stimulation. After a bleach pulse of 0.25 s, almost all GFP-GR molecules associated with the array structure had been bleached (Fig. 5, B and C). When irradiation of the structure was discontinued, GFP-GR fluorescence was again detected in association with the array structure within 2 s. There is a minimum 1.6-s delay between the end of the bleaching pulse and acquisition of the first image on the Leica confocal instrument (Exton, PA). Thus, the first image collected immediately after bleaching (Fig. 5C) is actually 1.6 s after bleaching. The very small amount of GFP-GR visualized in this image probably represents rebinding in this first 1.6-s period.
13. For FLIP experiments (Fig. 5, G to O), the 488- and

514-nm laser line beam of light was focused in the nucleus of living, hormone-treated cells at a distance from the position of the MMTV array (Fig. 5G). After collecting an initial complete image of the nucleus, the distant position was repeatedly irradiated as follows: 1 s of irradiation was followed by 1 s with no light, and then a full nuclear image was recorded with low-intensity excitation. This regimen was repeated for a total elapsed time of 1 to 2 min.

14. H. Richard-Foy and G. L. Hager, *EMBO J.* **6**, 2321 (1987); M. G. Cordingley, A. T. Riegel, G. L. Hager, *Cell* **48**, 261 (1987); T. K. Archer, P. Lefebvre, R. G. Wolford, G. L. Hager, *Science* **255**, 1573 (1992); G. Fragoso, S. John, M. S. Roberts, G. L. Hager, *Genes Dev.* **9**, 1933 (1995); G. Fragoso and G. L. Hager, *Methods* **11**, 246 (1997); C. L. Smith and G. L. Hager, *J. Biol. Chem.* **272**, 27493 (1997); G. Fragoso, W. D. Pennie, S. John, G. L. Hager, *Mol. Cell. Biol.* **18**, 3633 (1998).
15. T. M. Fletcher et al., in preparation.
16. S. Hahn, *Cell* **95**, 579 (1998); A. J. Berk, *Curr. Opin. Cell Biol.* **11**, 330 (1999).
17. J. Ellenberg, in preparation.
18. R. Heim and R. Y. Tsien, *Curr. Biol.* **6**, 178 (1996); D. A. De Angelis, G. Miesenbock, B. V. Zemelman, J. E. Rothman, *Proc. Natl. Acad. Sci. U.S.A.* **95**, 12312 (1998).
19. M. C. Ostrowski, H. Richard-Foy, R. G. Wolford, D. S. Berard, G. L. Hager, *Mol. Cell. Biol.* **3**, 2045 (1983).

16 November 1999; accepted 21 December 1999

Dopaminergic Loss and Inclusion Body Formation in α -Synuclein Mice: Implications for Neurodegenerative Disorders

Eliezer Masliah,^{1,2*} Edward Rockenstein,¹ Isaac Veinbergs,² Margaret Mallory,¹ Makoto Hashimoto,¹ Ayako Takeda,^{1,3} Yutaka Sagara,² Abbyann Sisk,² Lennart Mucke⁴

To elucidate the role of the synaptic protein α -synuclein in neurodegenerative disorders, transgenic mice expressing wild-type human α -synuclein were generated. Neuronal expression of human α -synuclein resulted in progressive accumulation of α -synuclein—and ubiquitin-immunoreactive inclusions in neurons in the neocortex, hippocampus, and substantia nigra. Ultrastructural analysis revealed both electron-dense intranuclear deposits and cytoplasmic inclusions. These alterations were associated with loss of dopaminergic terminals in the basal ganglia and with motor impairments. These results suggest that accumulation of wild-type α -synuclein may play a causal role in Parkinson's disease and related conditions.

Human α -synuclein is a 140-amino acid molecule (1) that is encoded by a gene on chromosome 4 (2) and has homology to rat and *Torpedo* α -synuclein and songbird synelfin (3). Although the precise function of the synuclein superfamily of peptides is still unknown, several lines of evidence suggest potential roles in synaptic function and neural plasticity (3, 4). Human α -synuclein was originally isolated from plaques of Alzheimer's disease brains as a 19-kD protein precursor of the highly hydrophobic 35-amino acid metabolite, nonamyloid component (NAC) of plaques (1). The NAC peptide can self-aggregate into fibrils and induces aggregation of the β -amyloid peptide (5).

α -Synuclein is highly abundant in presynaptic terminals (4) and in Lewy bodies (6), neuronal inclusions that are found in diverse human neurodegenerative disorders including the Lewy body variant of Alzheimer's disease, diffuse Lewy body disease, and Parkinson's disease (7). Rare cases of familial Parkinson's disease have recently been linked to point mutations in α -synuclein (8); however, most neurodegenerative disorders with Lewy bodies are associated with abnormal accumulation of wild-type, not mutant, α -synuclein (6, 9).

To elucidate the role of α -synuclein accumulation in the pathogenesis of neurodegenerative disorders with Lewy bodies, we generated

and analyzed α -synuclein transgenic mice. In these mice, wild-type human α -synuclein was expressed under the regulatory control of the platelet-derived growth factor- β (PDGF- β) promoter (Fig. 1A) (10). This promoter was chosen because it has been successfully used to target the expression of other human proteins to neurons in transgenic models of neurodegenerative disease (11). In all lines of transgenic mice with human α -synuclein mRNA expression in the brain (Fig. 1, B and C), cerebral human α -synuclein expression was also detect-

ed at the protein level (Fig. 1, E and F). Mice from line D consistently had the highest levels of human α -synuclein mRNA (Fig. 1C) and protein (Fig. 1F). Lines A, B, M, and C had low to intermediate levels of transgene expression (Fig. 1, C and F).

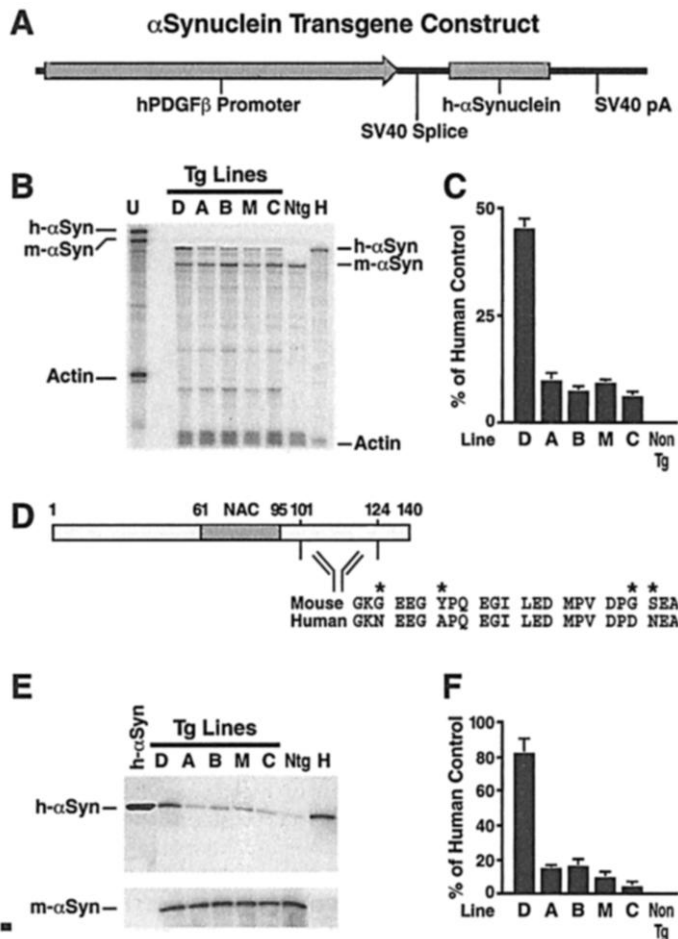
To characterize the effects of human α -synuclein expression in neurons, we compared transgenic mice from lines A ($n = 6$), B ($n = 8$), C ($n = 17$), D ($n = 15$), and M ($n = 6$) with age-matched nontransgenic controls ($n = 22$). By 2 months of age, transgenic mice

from all lines had prominent intraneuronal inclusions (nuclear and cytoplasmic) that were strongly immunoreactive with antibodies to human (Fig. 2B), but not mouse (Fig. 2E), α -synuclein. The antibody to human α -synuclein also recognized the characteristic intracytoplasmic inclusions found in Lewy body disease (Fig. 2C). Human α -synuclein-immunoreactive inclusions were most abundant in transgenic mice from the highest expresser line (Figs. 2B and 3A) and were not detected in nontransgenic controls (Fig. 2A). In the transgenic mice, the inclusions were most frequently seen in neurons in the deeper layers of the neocortex (Fig. 2B), the CA3 region of the hippocampus, and the olfactory bulb (12) and occasionally in the substantia nigra (Fig. 2, G and H). These regions are also typically affected in patients with Lewy body disease (6).

Degeneration of dopaminergic neurons in the substantia nigra results in Parkinson's disease and is frequently preceded by the formation of Lewy bodies. To assess whether these cells develop human α -synuclein-positive inclusions in our transgenic mice, we double-immunolabeled brain sections with antibodies to human α -synuclein and to tyrosine hydroxylase (TH) (13), which is required for the synthesis of dopamine. TH-positive neurons in the substantia nigra displayed abnormal accumulations of α -synuclein (Fig. 2H). Consistent with observations in humans with Lewy body disease (6, 7), the inclusions in the transgenic mice were accompanied by occasional human α -synuclein-immunoreactive neuritic processes (Fig. 2I) and were colabeled (13) with an antibody to ubiquitin (Fig. 2J).

We then characterized the ultrastructural features of the human α -synuclein-positive neuronal inclusions by electron microscopy (4, 14). In contrast to nontransgenic controls (Fig. 4, A and B), neurons of high-expresser human α -synuclein mice (2 to 3 months of age) showed electron-dense deposits (0.1 to 0.25 μ m in diameter) associated with the rough endoplasmic reticulum (Fig. 4, C and D). Larger electron-dense deposits (0.5 to 1 μ m in diameter) with a dense core were observed in neuronal nuclei (Fig. 4, E and F). Interestingly, other synaptic proteins also accumulate in neuronal nuclei in other neurodegenerative conditions. For instance, fibrillar aggregates of huntingtin are found in the nucleus of affected neurons in

Fig. 1. Characterization of α -synuclein expression in human α -synuclein transgenic mice. (A) Human PDGF- β promoter-driven transgene encoding wild-type human α -synuclein. h, human; pA, polyadenylation signal. (B) Representative autoradiograph showing cerebral α -synuclein mRNA levels in transgenic (Tg) mice of different lines, a nontransgenic (Ntg) mouse, and a human (H) without neurological disease. The frontoparietal cortex was analyzed by ribonuclease protection assay as described (22) with RNA probes specific for the entire coding sequence of human α -synuclein (h α -syn, GenBank accession number L08850) or for a segment of murine α -synuclein (m α -syn, GenBank accession number AF044672). The left-most lane shows signals of undigested (U) radiolabeled RNA probes; the other lanes contained the same RNA probes plus brain RNA samples digested with ribonucleases. Protected mRNAs are shown on the right. (C) PhosphorImager (Becton-Dickinson) analysis of human α -synuclein mRNA signals (expressed as percent of human control). The highest level of transgene expression was detected in mice from line D ($n = 3$) and intermediate to low levels were observed in lines M, A, B, and C ($n = 3$ mice per line). No human α -synuclein signal was detected in nontransgenic (Non Tg) mice ($n = 4$). Bars represent means \pm SEM. (D) Schematic representation of the α -synuclein region from which the human- and mouse-specific peptides were selected for generation of polyclonal antibodies. Mismatched amino acids are labeled with an asterisk. These antibodies were generated by Research Genetics (Huntsville, AL) as described (4) and affinity-purified with the AminoLink Kit (Pierce, Rockford, IL) with the immunogen. Single-letter abbreviations for the amino acid residues are as follows: A, Ala; D, Asp; E, Glu; G, Gly; I, Ile; K, Lys; L, Leu; M, Met; N, Asn; P, Pro; Q, Gln; S, Ser; V, Val; and Y, Tyr. (E) Western blot analysis (10 μ g protein per lane) with affinity-purified human- and mouse-specific α -synuclein antibodies was performed as described (4). The human-specific antibody recognized a 19-kD band, consistent with human α -synuclein, in the transgenic mice and in the human control. Only minimal cross-reactivity with mouse α -synuclein was seen in nontransgenic mice. In contrast, the murine-specific antibody recognized endogenous α -synuclein in transgenic and nontransgenic mice, with only a faint band noted in the human control. (F) PhosphorImager analysis of human α -synuclein signals (background values subtracted) from semiquantitative Western blots revealed the highest cerebral levels of human α -synuclein expression in mice from line D ($n = 3$) and intermediate to low levels in lines M, A, B, and C ($n = 3$ mice per line). The signal obtained in nontransgenic mice ($n = 4$) was considered background. Results were expressed as percent immunoreactivity of normal human control ($n = 3$). Bars represent means \pm SEM.



ed at the protein level (Fig. 1, E and F). Mice from line D consistently had the highest levels of human α -synuclein mRNA (Fig. 1C) and protein (Fig. 1F). Lines A, B, M, and C had low to intermediate levels of transgene expression (Fig. 1, C and F).

To characterize the effects of human α -synuclein expression in neurons, we compared transgenic mice from lines A ($n = 6$), B ($n = 8$), C ($n = 17$), D ($n = 15$), and M ($n = 6$) with age-matched nontransgenic controls ($n = 22$). By 2 months of age, transgenic mice

¹Department of Neurosciences, ²Department of Pathology, University of California San Diego, La Jolla, CA 92093-0624, USA. ³Department of Psychiatry, Yokohama City University, School of Medicine, 3-9 Fukuura, Kanazawa-ku, Yokohama 236, Japan. ⁴Gladstone Institute of Neurological Disease and Department of Neurology, University of California San Francisco, Post Office Box 419100, San Francisco, CA 94141-9100, USA.

*To whom correspondence should be addressed. E-mail: emaslah@ucsd.edu

REPORTS

huntingtin transgenic mice and in patients with Huntington's disease (15).

In 9- to 11-month-old α -synuclein transgenic mice, larger electron-dense cytoplasmic inclusions (2 to 5 μ m in diameter) were identified that were composed of fine granular material and contained clear vacuoles (50 to 100 nm in diameter) but no fibrillar elements (Fig. 4, G

and H). Immunogold electron microscopic analysis confirmed that these structures contained human α -synuclein immunoreactivity (Fig. 4H, inset). Control experiments in which sections from transgenic mice were incubated in the absence of primary antibody showed no immunogold labeling associated with inclusions (12). Nuclear or cytoplasmic inclusions such as those

depicted in Fig. 4, C to H, were not observed in nontransgenic controls or transgenic mice expressing other amyloidogenic proteins directed by the same promoter (11, 14).

The cytoplasmic neuronal inclusions in human α -synuclein transgenic mice resemble Lewy bodies in humans in some respects but not in others. Similarities include their locations

Fig. 2. Expression of α -synuclein immunoreactivity and neuropathological alterations in human α -synuclein transgenic mice. Brain sections from 3-month-old nontransgenic (A and D) and transgenic (B, E, and G to J) mice from line D and a human with Lewy body disease (C and F) were immunostained with an antibody to human α -synuclein (A to C and G to J) or murine α -synuclein (D to F) and imaged by light (A to G, and I) or confocal (H and J) microscopy. In nontransgenic mice, no human α -synuclein immunoreactivity was observed (A), whereas in the temporal neocortex of the transgenic mouse (B) and the human (C) there was intense α -synuclein immunoreactivity in nerve terminals and intracytoplasmic inclusions (arrows). The antibody to murine α -synuclein immunostained only the neuropil; there was no immunostaining of inclusions in the mice [(D) and (E)] or of the Lewy bodies or synapses in the human tissue (F). (G) Occasional human α -synuclein-immunoreactive structures (arrows) were observed in the cytoplasm of neurons in the substantia nigra pars compacta of transgenic mice. (H) Double labeling for human α -synuclein and TH revealed inclusion bodies (arrow) in dopaminergic neurons in the substantia nigra of the transgenic mouse. (I) Human α -synuclein-immunoreactive neuritic processes (arrows) were observed in the CA3 region of the hippocampus in transgenic mice. (J) Double labeling of transgenic brain sections revealed that some human α -synuclein-immunoreactive inclusions (red) were also ubiquitin-positive (green). Colabeled inclusions are seen in orange-yellow (arrow). Original magnification, $\times 295$ (A to G), $\times 830$ (H to J).

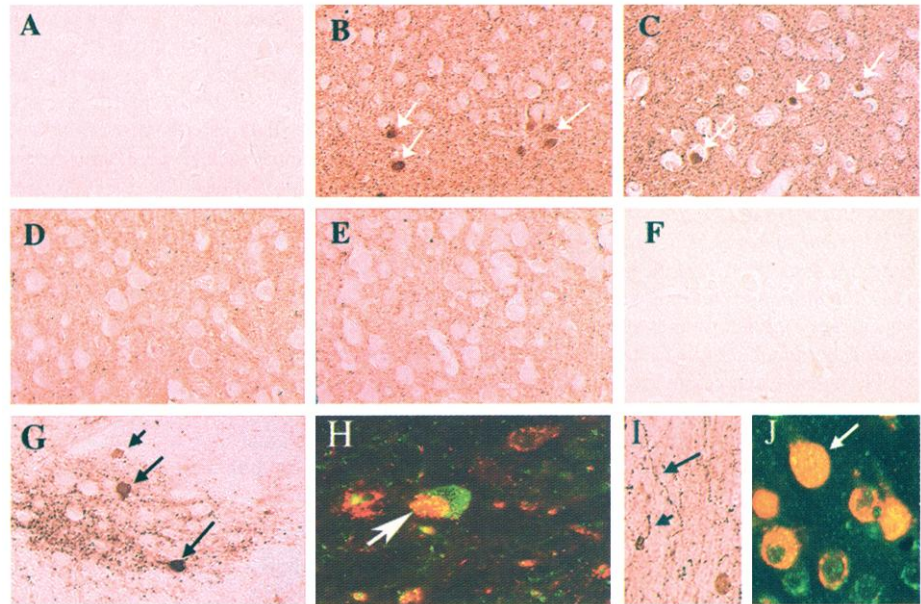
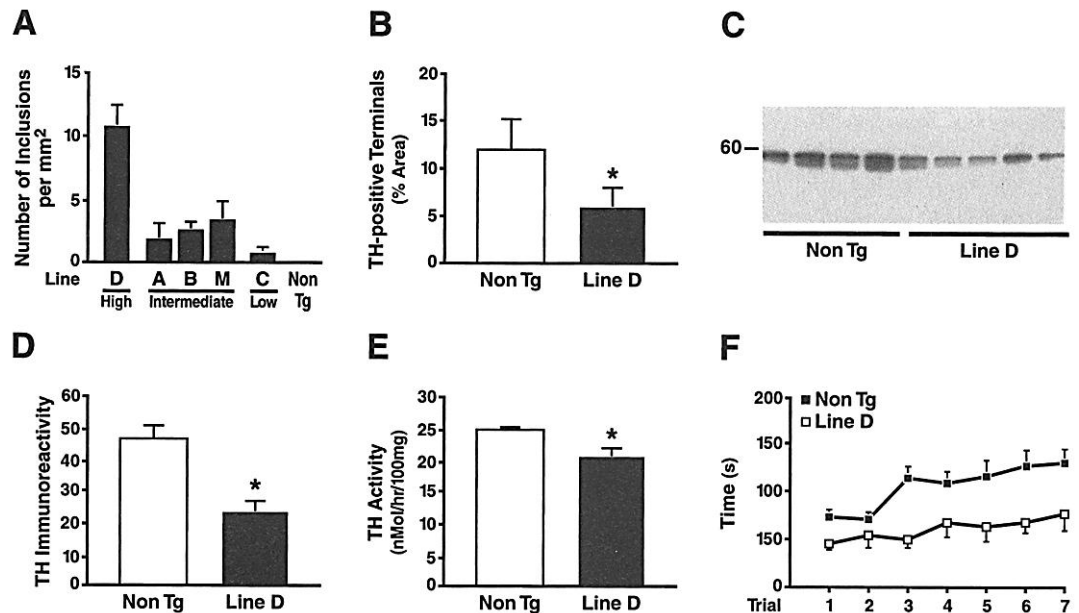


Fig. 3. A high number of neuronal inclusions are associated with the development of dopaminergic and motor deficits. (A) The density of human α -synuclein-immunoreactive neuronal inclusions in the cingulate cortex was determined (13) in 3- to 4-month-old transgenic mice from lines D ($n = 8$), M ($n = 3$), A ($n = 6$), B ($n = 4$), and C ($n = 7$) and in age-matched nontransgenic controls ($n = 8$). The highest and lowest numbers of inclusion bodies were found in the highest expresser (line D) and lowest expresser (line C) transgenic lines, respectively. (B) The density of TH-positive terminals in the striatum (13) was significantly lower in 12-month-old transgenic mice from line D than in age-matched nontransgenic controls ($n = 8$ mice per group; $*P < 0.05$ by unpaired two-tailed Student's t test). (C) Western blot (23) demonstrating striatal TH levels in transgenic mice from line D and nontransgenic controls at 12 months of age. (D) Analysis of TH bands with the ImageQuant software (23) confirmed that striatal TH levels were significantly lower in transgenic mice than in nontransgenic controls ($n = 5$ mice per group; $*P < 0.005$ by unpaired two-tailed Student's t test). (E) Striatal TH activity



(24) was also significantly lower in 12-month-old transgenic mice from line D than in nontransgenic littermates ($n = 5$ mice per group; $*P < 0.03$ by unpaired two-tailed Student's t test). (F) Rotorod testing (18) revealed a significant decrease in motor performance ($P < 0.01$ for genotype effect by repeated-measures analysis of variance) in 12-month-old transgenic mice from line D compared with nontransgenic littermates ($n = 10$ mice per group). All quantitative data represent group means \pm SEM.

in the deep layers of the neocortex and in dopaminergic neurons of the substantia nigra and their reactivity with antibodies to human α -synuclein or ubiquitin. They differ from human Lewy bodies in that they are less circumscribed, are present in the nucleus, and lack fibrillar components (6, 7). It is unclear why no fibrillar structures were detected in association with the electron-dense inclusions in transgenic mice. Conceivably, additional stress conditions, such as formation of oxygen free radicals, are necessary to promote fibrillar aggregation of human α -synuclein (16). This situation may be similar to that encountered in human amyloid protein precursor transgenic mice, where there is no formation of neurofibrillary tangles or paired helical filaments despite extensive deposition of amyloid (14).

Because motor deficits in Lewy body disease are associated with degeneration of nigral dopaminergic neurons projecting to the striatum (17), we further evaluated the integrity of the dopaminergic system. The density of TH-positive neurons in the substantia nigra was similar in all five lines of transgenic mice and in nontransgenic controls (12). However, TH-positive nerve terminals within the stri-

tum were significantly reduced in transgenic mice from the highest expresser line as compared with nontransgenic littermates (Fig. 3B) and lower expresser lines (12). Transgenic mice also had lower striatal TH levels by Western blot analysis (Fig. 3, C and D) and lower striatal levels of TH enzymatic activity (Fig. 3E) than nontransgenic controls. Thus, abnormal accumulation of human α -synuclein may lead to injury of nerve terminals and synapses in the absence of overt neuronal loss.

To determine if loss of dopaminergic input to the striatum in transgenic mice is associated with Parkinson's disease-related neurological impairments, we examined the mice with the rotorod test (18, 19). Compared with nontransgenic littermate controls, transgenic mice from the high-expresser line D showed significant deficits in motor performance (Fig. 3F). The loss of dopaminergic terminals and motor abnormalities in human α -synuclein transgenic mice support the general hypothesis that intraneuronal accumulation of amyloidogenic synaptic proteins can elicit morphological and functional impairments of the central nervous system (20).

Because the dopaminergic and behavioral deficits were detected only in the high-expresser line and not in low-expresser lines (12), these findings will need to be confirmed in additional high-expresser lines. Although the highest expresser line clearly had more human α -synuclein- and ubiquitin-immunoreactive neuronal inclusions than the other transgenic lines, these inclusions were observed in all transgenic lines analyzed (Fig. 3A). It is conceivable that a critical threshold of α -synuclein accumulation is required for dopaminergic and behavioral deficits to become detectable. Alternatively, the formation of neuronal inclusions and the development of neuronal deficits may not be linked in a causal chain. Evidence for such a dissociation has been obtained in models of polyglutamine-induced neurodegenerative disorders (21). In any case, the similarities between neurodegenerative diseases with Lewy bodies and the alterations elicited in human α -synuclein transgenic mice suggest that increased expression or intracellular accumulation of wild-type α -synuclein may play a key role in the pathogenesis of these conditions.

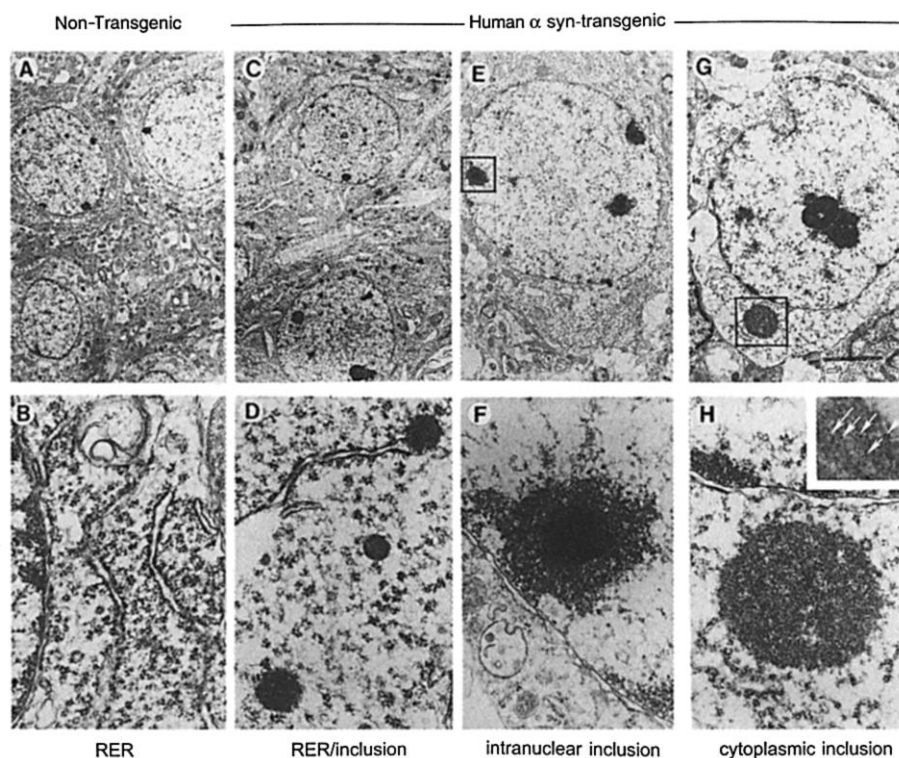


Fig. 4. Ultrastructural analysis of neuronal alterations in human α -synuclein transgenic mice (line D). Upper panels show low magnification (original magnification, $\times 2500$) and lower panels high magnification ($\times 15,000$) views of neurons from the cingulate cortex. Boxed areas in upper panels (E and G) indicate areas shown in lower panels (F and H). (A and B) Normal appearance of neuronal structures in a 3-month-old nontransgenic control. RER, rough endoplasmic reticulum. (C and D) Electron-dense inclusions in the RER in a 3-month-old transgenic mouse. (E and F) Nuclear inclusions in a 3-month-old transgenic mouse. The dense cores of these abnormal deposits distinguish them from the nuclear chromatin condensations seen in (A). (G and H) Electron-dense inclusions composed of fine granular material in the neuronal cytoplasm of an 11-month-old transgenic mouse. Immunogold electron microscopic analysis (4) of similar deposits in a different transgenic mouse (inset, H) confirmed that such electron-dense material contained human α -synuclein immunoreactivity (arrows). Bar, 5 μ m.

References and Notes

1. K. Ueda et al., *Proc. Natl. Acad. Sci. U.S.A.* **90**, 11282 (1993); R. Jakes, M. G. Spillantini, M. Goedert, *FEBS Lett.* **345**, 27 (1994).
2. X. Chen et al., *Genomics* **26**, 425 (1995).
3. D. F. Clayton and J. M. George, *Trends Neurosci.* **21**, 249 (1998).
4. A. Iwai et al., *Neuron* **14**, 467 (1994).
5. M. Yoshimoto et al., *Proc. Natl. Acad. Sci. U.S.A.* **92**, 9141 (1995).
6. M. G. Spillantini et al., *Nature* **388**, 839 (1997); A. Takeda et al., *Am. J. Pathol.* **152**, 367 (1998); K. Wakabayashi, K. Matsumoto, K. Takayama, M. Yoshimoto, H. Takahashi, *Neurosci. Lett.* **239**, 45 (1997).
7. K. Kosaka, *Acta Neuropathol.* **42**, 127 (1978); D. W. Dickson et al., *Acta Neuropathol.* **78**, 572 (1989).
8. M. H. Polymeropoulos et al., *Science* **276**, 2045 (1997); R. Kruger et al., *Nature Genet.* **18**, 106 (1998).
9. J. Q. Trojanowski and V. M. Lee, *Arch. Neurol.* **55**, 151 (1998).
10. A 1480-base pair (bp) fragment of 5'-flanking region of the human PDGF- β chain gene was isolated from the psisCAT plasmid (a gift from T. Collins, Harvard Medical School) and placed upstream of a Not I-Sal I fragment consisting from 5' to 3' of an SV40 splice, 423 bp of human cDNA encoding full-length wild-type α -synuclein, and SV40 sequence from the pCEP4 vector (Invitrogen) providing a polyadenylate signal. The resulting fusion gene was freed of vector sequences, purified, and microinjected into one-cell embryos (C57BL/6 \times DBA/2 F₂) according to standard procedures. Thirteen transgenic founders were identified by polymerase chain reaction (PCR) analysis of tail DNA. Genomic DNA was extracted and amplified in 30 cycles (93°C for 30 s, 57°C for 30 s, 72°C for 1.5 min) with a final extension at 72°C for 5 min. Primers were as follows: 5'-CCAGCGGCCGCTCTAGAAC-TAGTG (sense) and 5'-CCAGTCGACCGGTCATGGCT-GCCG (antisense).
11. D. Games et al., *Nature* **373**, 523 (1995).
12. E. Masliah et al., data not shown.
13. Double-immunolabeling studies were performed on 40- μ m-thick vibratome sections, which were first incubated overnight at 4°C with a human α -synuclein-specific antibody (1:1000) (Fig. 1, D to F), followed by detection

Neuroimaging Evidence for Dissociable Forms of Repetition Priming

R. Henson,^{1,2*} T. Shallice,^{2,3} R. Dolan^{1,4}

Repetition priming has been characterized neurophysiologically as a decreased response following stimulus repetition. The present study used event-related functional magnetic resonance imaging to investigate whether this repetition-related response is sensitive to stimulus familiarity. A right fusiform region exhibited an attenuated response to the repetition of familiar stimuli, both faces and symbols, but exhibited an enhanced response to the repetition of unfamiliar stimuli. Moreover, both repetition effects were modulated by lag between successive presentations. Further experiments replicated the interactions between repetition, familiarity, and lag and demonstrated the persistence of these effects over multiple repetitions. Priming-related responses are therefore not unitary but depend on the presence or absence of preexisting stimulus representations.

Repetition priming is one of the basic forms of memory in higher nervous systems. It has been studied extensively by cognitive psychologists, often indexed behaviorally as faster reaction times or improved identification accuracy following repetition (1). A well-established neurophysiological index of repetition priming is a relative decrease in neural firing with repeated stimulus presentations, referred to as "repetition suppression" (2), as found, for example, in inferotemporal regions of the monkey cortex (3). Analogous decreases in the hemodynamic response following stimulus repetition have been reported within the human extrastriate cortex in functional imaging studies (4). These imaging studies have typically used familiar stimuli, such as common words or pictures of identifiable objects. In the present imaging study, we examined whether repetition priming effects are modulated by stimulus familiarity. By familiarity, we refer to whether or not a representation of the stimulus existed before scanning.

In four experiments conforming to the same basic paradigm, we used functional magnetic resonance imaging (fMRI) (5) to measure the event-related hemodynamic response to brief visual stimuli (Fig. 1). Participants (6) viewed a baseline image that was replaced by either a face (experiments 1 and 3) or a symbol (experiments 2 and 4). Each stimulus was either familiar (a famous face or a meaningful symbol) or unfamiliar (a nonfamous face or a meaningless symbol) and was presented twice (experi-

ments 1 and 2) or five times (experiments 3 and 4) in a randomly intermixed design. Participants were required to press a key only if the stimulus was a prespecified target, so that the events of interest, the nontarget stimuli, were uncontaminated by motor response requirements. This use of an indirect task removes any explicit requirement for differential attention to stimulus familiarity or repetition. After scanning, participants were shown the stimuli again and judged which could be identified (i.e., faces identified as famous or symbols identified as meaningful). Although the judgments were in good agreement, the differences allowed analyses to be individually tailored to participants' prior experience.

Experiments 1 and 2 employed a two-by-two factorial design in which the events of interest were first and second presentation of familiar (F1 and F2) and unfamiliar (U1 and U2) stimuli. We created statistical parametric maps of voxels exhibiting increased responses to stimulus presentation versus baseline (7). These voxels (which comprised mainly bilateral fusiform, right lateral occipital, and inferior frontal regions) were then used as a mask within which to identify brain regions sensitive to two planned, orthogonal comparisons: (i) regions showing greater responses to familiar than to unfamiliar stimuli, (F1 + F2) – (U1 + U2), and (ii) regions showing an interaction between familiarity and repetition, (F1 – F2) – (U1 – U2).

The only regions exhibiting a greater response to familiar than to unfamiliar faces were in the bilateral fusiform cortex (Fig. 2A), close to what has been referred to as the "face area" (8). The present results suggest that this region is sensitive to whether or not a face is recognized, perhaps reflecting activation of "face recognition units" (FRUs) (9). Similar bilateral fusiform regions, however [given the spatial smoothing of the data (5)], exhibited a greater

with the Tyramide Signal Amplification-Direct (Tyramide Red) system (1:100; NEN Life Sciences, Boston, MA). Sections were then incubated overnight with a monoclonal antibody (mAb) to TH (1:10; Roche Molecular Biochemicals), followed by incubation with a fluorescein isothiocyanate (FITC)-conjugated secondary antibody to mouse immunoglobulin G (IgG) (1:75; Vector Laboratories). The specificity of the primary antibodies was confirmed in control experiments in which sections were incubated with preimmune serum instead of primary antibody, or with primary antibody preabsorbed for 48 hours with a 20-fold excess of the peptide to which the antibody was raised, or in the absence of primary antibody. Other sections were double-immunolabeled with antibody to human α -synuclein (as above) and rabbit polyclonal antibody to ubiquitin (1:50 or 0.2 mg/ml; DAKO Corporation, Carpinteria, CA) detected with an FITC-conjugated secondary antibody to rabbit IgG (1:75; Vector Laboratories). To evaluate the integrity of presynaptic terminals and dopaminergic neurons, we double-immunolabeled sections with a mAb to synaptophysin (1:2500; Roche) (Tyramide Red detection system) and a mAb to TH (see above). Brain sections from mice to be compared in any given experiment were processed and immunolabeled in parallel. Three sections were analyzed per mouse, and four serial 2- μ m-thick optical sections were obtained per section. For each experiment, the linear range of the intensity of immunoreactive structures in control sections was determined with a MRC1024 (Bio-Rad) confocal microscope. This setting was then used for the collection of all images to be analyzed in the same experiment. Digitized images were transferred to a Power-PC Macintosh computer, and NIH Image 1.4 software was used to calculate the percent image area covered by immunoreactive terminals. The number of TH-positive neurons in the pars compacta of the substantia nigra was estimated essentially as described [A. Hsia et al., *Proc. Natl. Acad. Sci. U.S.A.* **96**, 3228 (1999)].

14. E. Masliah et al., *J. Neurosci.* **16**, 5795 (1996).
15. S. W. Davies et al., *Cell* **90**, 537 (1997).
16. M. Hashimoto et al., *Brain Res.* **799**, 301 (1998); M. Hashimoto et al., *Neuroreport* **10**, 717 (1999).
17. S. Gauthier and T. L. Sourkes, *Prog. Neuro-psychopharmacol. Biol. Psychiatry* **6**, 595 (1982).
18. Mice were evaluated as described (19) with a rotorod (San Diego Instruments, San Diego, CA). Initially, they were trained for five trials. During the subsequent test trials, mice were placed individually on the cylinder and the speed of rotation increased from 0 to 40 rpm over a period of 240 s. The length of time mice remained on the rod (fall latency) was recorded and used as a measure of motor function.
19. M. J. Forster and H. Lal, *Neurobiol. Aging* **20**, 167 (1999).
20. E. Masliah, *Neurosci. News* **1**, 14 (1998).
21. I. A. Klement et al., *Cell* **95**, 41 (1998); F. Saudou et al., *Cell* **95**, 55 (1998).
22. E. M. Rockenstein et al., *J. Biol. Chem.* **270**, 28257 (1995).
23. For Western blot analysis of TH levels, brains were homogenized and separated into cytosolic and particulate fractions as described (4). Twelve micrograms of cytosolic fraction per mouse were loaded onto 10% SDS-polyacrylamide gel electrophoresis gels followed by transfer of proteins onto Immobilon membranes and detection of TH with a mAb to TH (1:1000; Roche). Blots were incubated with horseradish peroxidase-coupled secondary antibody and developed with the chemiluminescence reagent (NEN). After exposure of blots to film, the density of bands was quantitated with the ImageQuant system (Molecular Dynamics, Sunnyvale, CA).
24. J. F. Reinhard, G.K. Smith, C.A. Nichol. *Life Sci.* **39**, 2185 (1986).
25. We thank S. Ordway and G. Howard for editorial assistance and M. Alford for technical assistance. Supported by NIH Grants AG5131 and AG10689 (to E.M.) and AG11385 (to L.M.) and the Spencer Family Foundation (to M.H.).

17 September 1999; 3 January 2000

¹Wellcome Department of Cognitive Neurology, Institute of Neurology, ²Institute of Cognitive Neuroscience and Department of Psychology, University College London, London WC1E 6BT, UK. ³Scuola Internazionale Superiore di Studi Avanzati, Via Beirut 2-4, 34014 Trieste, Italy. ⁴Royal Free and University College Medical School, Rowland Hill Street, London NW3 2PF, UK.

*To whom correspondence should be addressed. E-mail: r.henson@ucl.ac.uk